3D 프린팅 응용을 위한 내구성 있는 Polylactic Acid - 열가소성 폴리우레탄 탄성체 복합물의 합성

Xiaojie Zhang · Jianhua Xiao* · 김진국** · 오정석**,† · 이진호***,†

School of Materials Science and Engineering, Nanchang Hangkong University
*School of Chemistry and Chemical Engineering, Shanghai University of Engineering Science
**경상국립대학교 나노신소재융합공학과
***경상국립대학교 물리교육과
(2023년 5월 31일 접수, 2023년 8월 15일 수정, 2023년 8월 17일 채택)

Innovative Synthesis of Durable Polylactic Acid-Thermoplastic Polyurethane Elastomer Composites for Three-Dimensional Printing Applications

Xiaojie Zhang, Jianhua Xiao*, Jin Kuk Kim**, Jeong Seok Oh**,†, and Jinho Lee***,†

School of Materials Science and Engineering, Nanchang Hangkong University, Nanchang 330000, China
*School of Chemistry and Chemical Engineering, Shanghai University of Engineering Science, Shanghai 201620, China
**Department of Materials Engineering and Convergence Technology, Engineering Research Institute,
Gyeongsang National University, Jinju 52828, Korea
***Department of Physics Education and the Research Institute of Natural Science,
Gyeongsang National University, Jinju 52828, Korea
(Received May 31, 2023; Revised August 15, 2023; Accepted August 17, 2023)

초록: PLA와 열가소성 폴리우레탄(TPU) 간의 호환성을 향상시키기 위해 동적 반응을 통해 cardanol을 주요 백본 체인에 그래프팅하였다. Cardanol-grafted PLA(PLAC)/TPU 혼합 기반 필라멘트는 용융 압출을 사용하여 테스트되었고 PLAC 그래프팅 비율이 PLAC/TPU 혼합물의 유변학적 특성 및 열 변형과 3 차원 인쇄 부품의 기계적 특성에 미치는 영향을 조사하였다. Cardanol 농도가 증가함에 따라 유리 전이 온도가 감소하는 것을 확인하였고 differential scanning calorimetry 측정으로 결정성 감소가 관찰되어 PLA 와 TPU 간의 혼화성이 향상되었으며 결과적으로 PLAC/TPU 블렌드의 향상된 인성을 볼 수 있었다.

Abstract: The functionalization of polylactic acid (PLA) is examined by grafting cardanol onto its main backbone chain through a dynamic reaction to improve compatibility between PLA and thermoplastic polyurethane (TPU). Cardanol-grafted PLA (PLAC)/TPU blend-based filaments for fused deposition modeling are tested using melt extrusion. Effects of PLAC grafting ratio on the rheological properties and thermal transformation of the PLAC/TPU blends and the mechanical properties of three-dimensional-printed parts are investigated. A decrease in the glass transition temperature and crystallinity from differential scanning calorimetry are observed with increasing cardanol concentration, implying improved miscibility between PLAC and TPU and as a result, PLAC/TPU blends exhibit improved toughness.

Keywords: cardanol, polylactic acid, fused deposition modeling, 3D printing, dynamic reaction.

Introduction

Over the past few years, additive manufacturing (AM) technology has been employed in aerospace, automotive, archi-tecture, medical, education, and fashion applications[1] owing to its advantages of producing complex shapes in a time-efficient and cost-effective manner.[2] Several AM techniques, such as fused deposition modeling (FDM), stereolithography, inkjet printing, and selective laser sintering,[3] have been developed. Among them, FDM is the most commonly used technique[4-6] owing to its cost-effectiveness, versatility, ease of use, and cus-tomizability.

Polylactic acid (PLA) is a widely utilized raw material in FDM-based three-dimensional (3D)-printing processes because it offers numerous advantages, such as high strength and modulus, good processability, biodegradability, and barrier properties.[7] However, the applications of PLA are hindered by drawbacks, such as poor processability, small elongation at break, and poor impact strength.[8]

To overcome these drawbacks, the blending of PLA with poly(ε-caprolactone), poly(butylene adipate-co-terephthalate),[7,9] poly(butylene succinate),[10,11] thermoplastic polyurethane (TPU) elastomers, polypropylene/ethylene-propylene-diene rubber, polyester elastomers, ethylene-n-butyl acrylate-glycidyl methacrylate, poly-(ethylene-glycidyl methacrylate), and unsaturated aliphatic polyester elastomers have been studied. These combinations have been shown to improve the toughness of PLA,[12-14] and among them, TPU is considered a good candidate to facilitate the toughening of PLA owing to its unique flexibility, durability, toughness, and biocompatibility.[15,16] However, multiphase morphology that originates from immiscible systems formed between PLA and TPU weakens interfacial adhesion.[17] Consequently, the performance of such blends is limited. Nonetheless, enhanced compatibility between PLA and TPU can be realized using an additional plasticizer.

Cardanol is a by-product obtained during the processing of natural cashew shells. It is used as a plasticizer and antioxidant as well for improving the physico-mechanical properties in the polymer industry. Cardanol can be used as an interfacial compatibilizer via reactive compatibilization with the aid of the unsaturated side chains and phenyl hydroxyl.[18] In contrast to other interfacial compatibilizers, cardanol is an eco-friendly and cost-effective alternative for enhancing the interface interaction between PLA and TPU, while retaining the biocompatibility of the blends. Previous studies demonstrated the compatibilization of cardanol-grafted polypropylene/bamboo composites,[19] cardanol-grafted liquid isoprene rubber/silica composites,[20] and cardanol-grafted poly(acrylonitrile–butadiene–styrene) (ABS)/PLA blends.[21] However, studies on the compatibilization of cardanol-grafted PLA/TPU blends have not been conducted thus far.

In this study, first, cardanol-grafted PLA (PLAC) polymers were synthesized using dicumyl peroxide (DCP) to initiate free radical reactions between PLA and the unsaturated side chains of cardanol during a dynamic reaction in an extruder. The branched side chains of PLAC are expected to improve the miscibility with TPU macromolecules under heat and shear stress conditions during melt processing. Second, the rheological and thermal properties and 3D-printed parts of the PLAC/TPU blends were examined to evaluate the effectiveness of grafting. In addition, the percent grafting and chemical structure of PLAC were characterized.

We demonstrate that cardanol can function as a multifunctional additive in PLA/TPU blends by acting as a compatibilizer and plasticizer; consequently, the toughness of PLA can be effectively improved by dynamic reactive compatibilization. Moreover, the proposed method can be used to generate high-toughness and biochemical PLA-based filament for 3D printing.

Experimental

Materials. PLA was obtained from Dongguan Dezhijian Co. Ltd. (China). Cardanol was supplied by Shandong Jiaying Chemical Technology Co. Ltd. (China). DCP was purchased from Jiangsu Altertech Material Co. Ltd. (China). TPU (LM-95A) was acquired from The Lubrizol Corporation (USA). All the other chemicals and reagents were obtained from a local market.

Synthesis of PLAC Polymers. Precalculated amounts of PLA, cardanol (0, 0.5, 1, 3, and 5 wt%), and DCP (0.5 wt%)[22,23] were premixed at 1500 rpm/min and 25 ℃ in a high-speed mixer (HRS-0.5, Huanxin Technology, China). The PLA was dried for 24 h in a vacuum oven at 65 ℃ and 24 bar to remove moisture before compounding. Thereafter, the mixture was extruded using a corotation twin-screw extruder (SHJ-20C, Nanjing Giant Machinery, China). The rotation speed of the extruder was controlled at 10 rpm/min, and the extrusion temperature from the feeder to the die was set to 170/180/190/185/180/170 ℃. The extrudate was solidified in a water bath
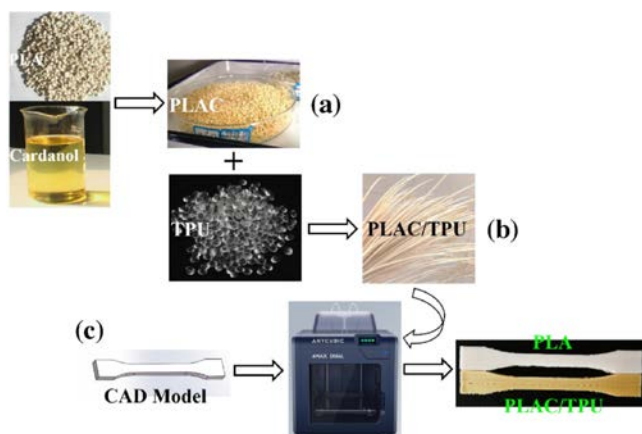

Figure 1. (a) Preparation of PLAC; (b) preparation of PLAC/TPU filaments; (c) FDM printing of PLA and PLAC/TPU dumbbell-shaped specimens.

Table 1. FDM-Printing Parameters

Parameters	Nozzle diameter (mm)	Layer thickness (mm)	Printing speed (mm/s)	Nozzle temperature (℃)	Bed temperature (℃)	Fill density (%)
Value	0.4	0.1	40	190	60	20

before granulation (Figure 1(a)). Thereafter, the PLAC polymer was dried under a vacuum at 80 ℃ to remove the absorbed water.

Preparation of PLAC/TPU Blends. The PLAC/TPU blends were obtained through the melt processing of PLAC and TPU in the twin-screw extruder, and the temperature from the feeder to the die was set to 170/180/190/185/180/170 ℃. The PLAC/TPU weight ratio was fixed at 70/30.[16] Filaments with a diameter of 1.75 ± 0.5 mm were obtained by adjusting the rotational speed of the winder (Figure 1(b)).

FDM Process. ISO527-2-2012 1BA type dumbbell-shaped specimens with a thickness of 4 mm were manufactured using an FDM 3D printer (4Max Pro2.0, Shenzhen Anycubic, China). The parameters of the FDM printer are listed in Table 1. Figure 1(c) shows the FDM-printing procedure for the specimens.

Characterization. Determination of Percent Grafting: The PLAC was extracted for 48 h with acetone in a Soxhlet apparatus to remove any physically bound or entrapped cardanol and DCP. The precipitate was dried at 70 ℃ in a vacuum oven until a constant weight was achieved.[24,25]

The percent grafting was calculated from the residual weight, as follows:

$$\text{Percent grafting (\%)} = \frac{\text{Weight of cardaonl grafted onto PLA}}{\text{Weight of grafted PLAC}} \times 100 \quad (1)$$

Gel Fraction: The PLAC was extracted using a Soxhlet extractor with toluene as the solvent. Before extraction, a certain amount of PLAC was packed with filter paper, and the system was refluxed for 12 h. The package was dried and weighed after the extraction. The extraction was repeated until no soluble residue was remaining in the package. The gel fraction was calculated using the following equation:[19]

$$\text{Gel fraction (\%)} = \frac{M_R - (M_T - M_P)}{M_P} \times 100 \quad (2)$$

where M_P is the weight of PLAC (g); M_T is the sum of the weights of PLAC and the filter paper before extraction (g); and M_R is the sum of the weights of residual PLAC and the filter paper after extraction (g).

Fourier Transform Infrared (FTIR) Spectroscopy: FTIR spectra were recorded on a VERTEX70 (Bruker, Germany) spectrometer in a range of 400-4000 cm^{-1}. The samples were purified by dissolving in refluxing acetone and toluene to remove the unreacted cardanol and DCP.

Rheological Properties: The rheological properties were measured at 190 ℃ and shear rates of 100-1500 s^{-1} using a capillary rheometer (MLW-400B, Changchun Intelligent Instrument and Equipment, China) and a die with $L/D = 10$ (length: 10 mm, diameter: 1 mm).[26,27]

The melt flow index (MFI)[28] was measured using an XNR-400C melt flow indexer (Jinhe Instruments, China). The test was performed at a uniform temperature of 190 ℃ with a load of 3.24 kg. A rod (100 g) was used as a plunger. The MFI value was the average value of at least five measurements.

Tensile Properties: The tensile strength and elongation at break were measured using a universal testing machine (YF-900, Yuanfeng, China) at a crosshead speed of 10 mm/min according to ISO-527-1-2021. The sample length between benchmarks was 50 mm. Medial values were obtained from at least five specimens of each blend.

Impact Measurement: The edgewise unnotched Charpy test was performed for all samples using the XJJ-50 Beam impact testing machine (Chengde Kecheng Testing Machine, China) according to ISO 179-1. At least three specimens were tested for each sample under the same conditions to ensure data reliability.

Thermal Analysis: Differential scanning calorimetry (DSC, DSC6200, NSK, Japan) was used for thermal analysis. The DSC program was set as follows. A temperature of 40 ℃ was maintained for 3 min. Thereafter, it was increased to 200 ℃ at 10 ℃/min, maintained for 5 min to remove any thermal history, decreased to -50 ℃ at 10 ℃/min, maintained for 5 min, and then increased to 200 ℃ at 10 ℃/min.[29] The TA Universal Analysis (v4.4A) software was used to analyze the data.

Results and Discussion

Effect of Cardanol Concentration on Grafting Ratio. PLAC was synthesized using a cardanol monomer and free radical initiator (DCP, 0.5 wt% of PLA) through a polymerization reaction. The steps involved in the grafting reaction are shown in
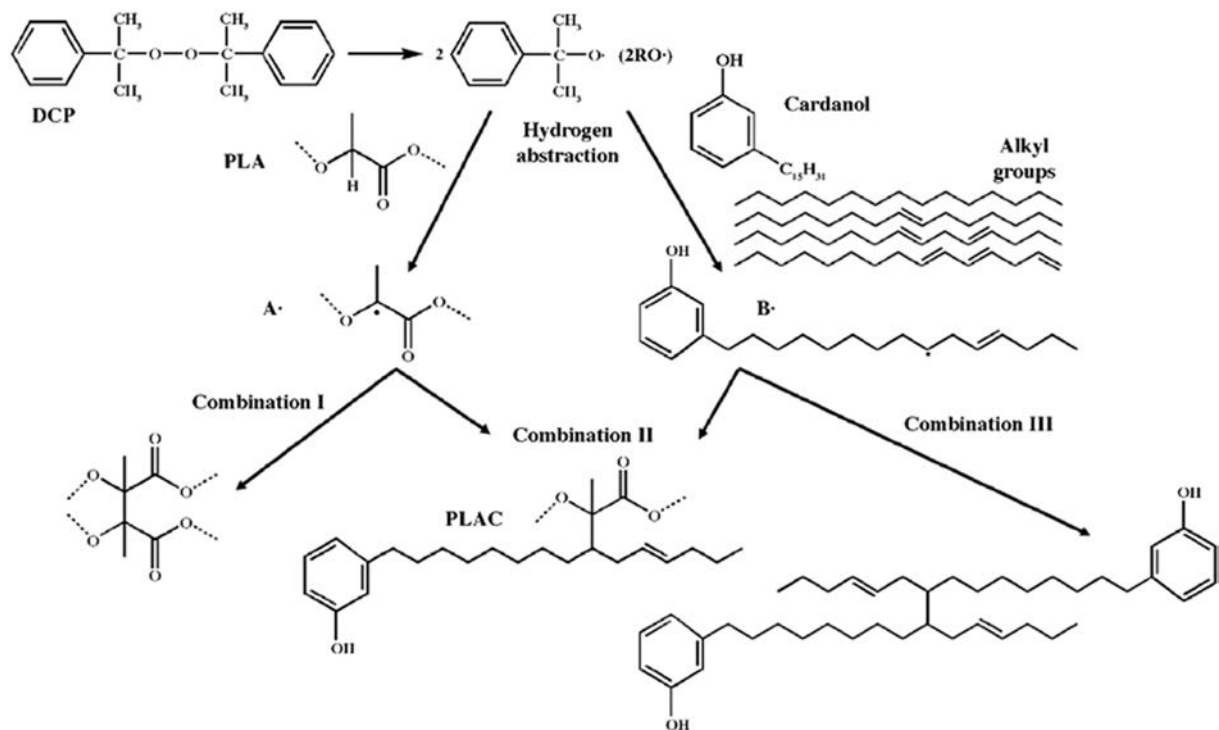
Figure 2. Proposed reaction mechanism of PLAC.

Figure 2. The reaction begins with the thermal homolytic scission of the oxygen–oxygen bonds of DCP to from peroxy radicals (RO·). These radicals can capture hydrogen at the α-carbon atom relative to the ester group and form a PLA macroradical (A·). Additionally, they can attack the unsaturated side chains of cardanol to form radicals (B·). After the PLA macroradical is generated, various termination reactions can occur through cardanol grafting or recombination along with other possible reactions. As shown in Figure 2, chain extension (crosslinking reaction) can occur through Combinations I and III during the grafting reaction. Cardanol grafting on the PLA macroradical occurs through Combination II. The movement of unsaturated side chains is hindered by the rigid phenyl groups of cardanol; therefore, cardanol grafted onto PLA does not crosslink during reactive extrusion. Hence, it is possible to obtain dimers or oligomers instead of crosslinked polymers.[19,30]

The cardanol concentration and percent grafting (the mass ratio of grafted cardanol to PLA) were investigated to qualitatively estimate the grafting degree of PLAC. Figure 3(a) shows that the percent grafting increases until a cardanol concentration of 1% and then becomes saturated because the reaction time and reaction sites on PLA and the DCP content are limited.[31] The reaction is initiated by DCP mainly owing to col-
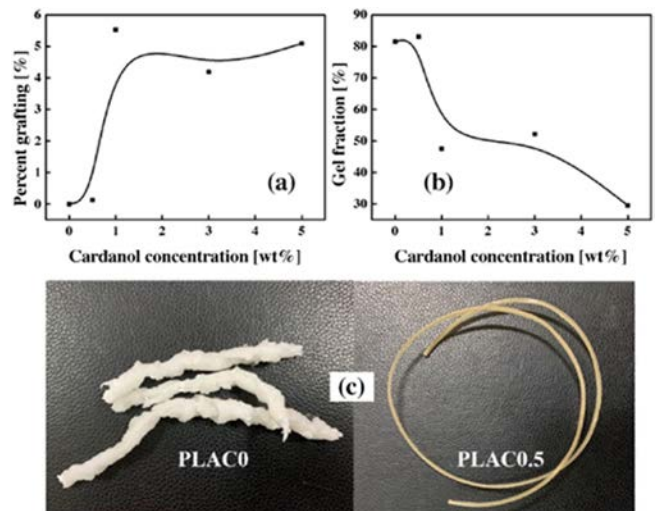

Figure 3. Effects of the cardanol concentration on (a) percent grafting and (b) gel fraction; (c) extruded filaments of PLAC0 and PLAC0.5.

lisions, and the probability of collisions significantly increases with the cardanol concentration. Accordingly, a higher cardanol concentration results in a higher grafting percentage. A crosslinking reaction between PLA macroradicals is inevitable during melt grafting extrusion initiated by a peroxide (Figure 2, Combination I). Gel fraction experiments were used to test
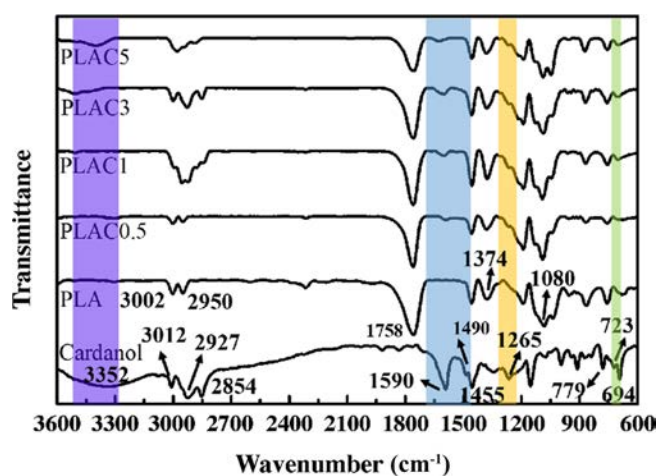
Figure 4. FTIR spectra of cardanol, PLA, and PLAC.

the crosslinking frequency of PLA macroradicals. As shown in Figure 3(b), the variations in the percent grafting and gel fraction with the cardanol concentration show opposite trends because the cardanol monomer is an efficient plasticizer for PLA.[32,33] The cardanol monomer can easily disperse into the PLA macromolecules and hinder the recombination reaction between PLA macroradicals. Therefore, the gel fraction decreases as the cardanol concentration increases. Figure 3(c) shows the extruded filaments of PLAC0 and PLAC0.5. A strong extrudate swelling phenomenon is observed, and foam-like structures are formed through the dominant crosslinking reactions owing to the absence of cardanol in PLAC034. Consequently, the stiffness characteristics of PLAC0 render it difficult to process and use for filament preparation for FDM. However, with the addition of cardanol, PLAC0.5 shows a smooth and uniform shape without extrudate swelling, as shown in Figure 3(c).

Characterization of PLAC. The grafting of cardanol onto the PLA macromolecules was confirmed by FTIR analysis, as shown in Figure 4. PLAC was purified to remove the unreacted cardanol and DCP by dissolving in refluxing acetone and toluene. The figure also shows the cardanol spectrum to identify and compare the absorption bands related to cardanol chemical bonds. In the cardanol spectrum, the strong and broad absorption peak at 3352 cm^{-1} (violet band in the figure) corresponds to the hydroxyl group. The peak at 3012 cm^{-1} is attributed to the unsaturated group (C=C-H) in the alkyl side chains. The characteristic peaks at 2927 and 2854 cm^{-1} correspond to methylene C-H and methyl C-H stretching, respectively. The peaks at 1590 (the skeletal vibration of aromatic (-C=C-) linkages), 1490, and 1455 cm^{-1} are associated with the vibration absorption of the benzene ring.[34] The peak at 1265 cm^{-1} indicates the presence of the C-O stretching aromatic ring. The ortho substitution in benzene nuclei is confirmed by the presence of the peak at 723 cm^{-1}. The vinyl vibrations at 694, 779, and 991-869 cm^{-1} are due to side chain (-C=C-) double bonds.[35] The PLA characteristic spectral peaks at 1758, 3002, 2950, and 1080 cm^{-1} correspond to C=O, -CH$_3$ asymmetric, -CH$_3$ symmetric, and C-O, respectively. The peaks at 1455 and 1374 cm^{-1} correspond to -CH$_3$ asymmetric and -CH$_3$ symmetric blending frequencies, respectively.[36] The PLAC spectrum also shows evident absorption peaks at 3352 and 1590 cm^{-1}, which are assigned to the stretching vibration of the phenolic hydroxyl group and skeletal vibration of the benzene ring, respectively; these are mainly due to the presence of cardanol. Additionally, the peaks at approximately 1250-1600 cm^{-1} (yellow and blue bands in the figure) correspond to the in-plane bending of the aromatic ring. Based on the above-mentioned analysis, the
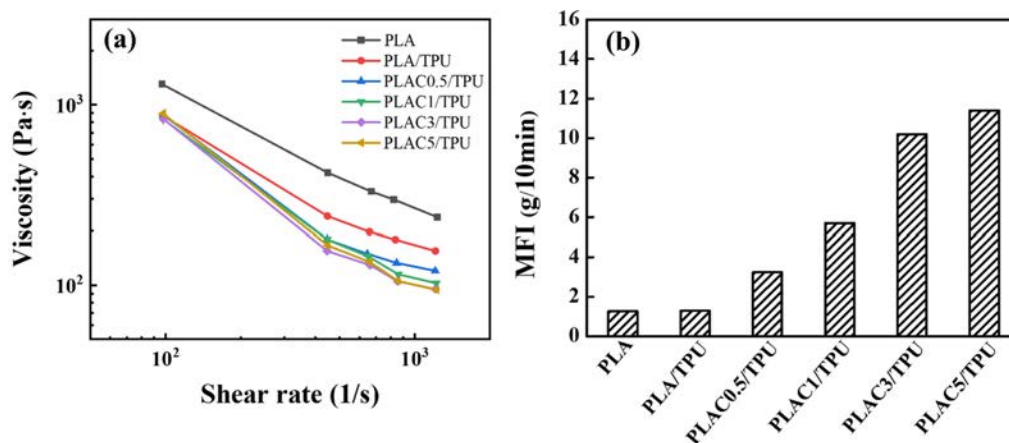

Figure 5. (a) Steady shear rheology curve of viscosity as a function of shear rate for PLAC/TPU blends at 190 ℃; (b) MFI of PLAC/TPU blends.

grafting reaction occurs through the side chain of cardanol in the presence of DCP. In addition, the phenolic group does not participate in the reaction and remains intact.[37]

Characterization of PLAC. The rheological properties and MFIs of various PLAC/TPU blend filaments were investigated, considering the importance of the melt viscosity of the polymer filaments for the feeding performance.[38,39] The viscosity (η) versus the shear rate (γ) at 190 ℃ are shown in Figure 5(a). For all blends, η decreases as γ increases, indicating that the blends behave as pseudoplastic or shear-thinning fluids under the experimental conditions.

The relationship between η and γ is defined by the power-law model,[26,40] as follows:

$$\eta = K\gamma^{n-1} \text{ or } \log\eta = \log K + (n-1)\log\gamma, \qquad (3)$$

where K is the consistency index, and n is the power-law index. Note that $n = 1$ corresponds to Newtonian behavior, and n is less than 1 for pseudoplastic fluids. Figure 5(a) shows that the behavior of the PLAC/TPU blends closely resembles the power-law behavior at the investigated shear rate. The power-law parameters for all blends are listed in Table 2. As the cardanol concentration in PLAC increases, the shear thinning in the melt PLAC/TPU blends becomes stronger, and n decreases. The rheological behavior of the blends is influenced by the cardanol concentration. The alkyl side chains of PLAC and dissociative cardanol in the blends can weaken the PLAC–PLAC and TPU–TPU interactions (hydrogen bonds), respectively. Therefore, the mobility of the macromolecules is higher under the same processing conditions, and the blends exhibit a stronger shear-thinning behavior. Therefore, 5 wt% is the maximum cardanol concentration in PLAC (PLAC5). At cardanol concentrations higher than 5 wt%, the extrudate behavior is similar to that of a Newtonian liquid. Hence, it is difficult to form filaments for FDM.

Figure 5(b) shows the MFIs of the PLAC/TPU blends as a function of the cardanol concentration. The MFI is inversely

Table 2. Power-law Parameters of PLAC/TPU Blends

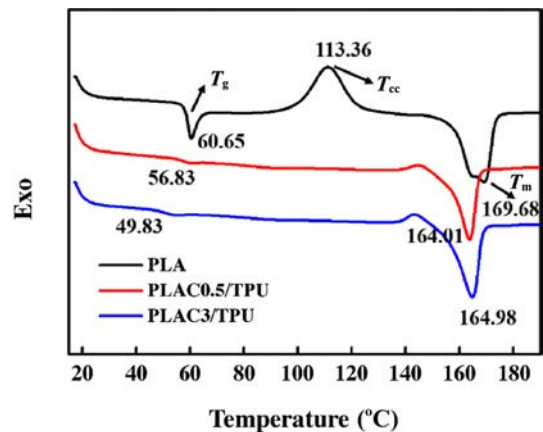| Specimen	Power-law index	Consistency index $(K, Ns^n/m^2) \times 10^4$
PLA	0.321	2.83
PLA/TPU	0.292	2.08
PLAC0.5/TPU	0.172	4.65
PLAC1/TPU	0.140	3.96
PLAC3/TPU	0.101	4.65
PLAC5/TPU	0.075	5.67

Figure 6. DSC thermograms of PLA and PLAC/TPU blends.

proportional to the viscosity of the polymer melts. The branching and crosslinked structures can cause a low MFI.[19] The MFI (melt viscosity) increases with the cardanol concentration, which is the same trend as that observed for the rheological properties. The MFI increases from 1.3 to 11.40 g/10 min as the cardanol concentration increases from 0 to 5 wt%. As the cardanol concentration increases further, the percent grafting increases, and the possibility of crosslinking decreases, which decreases the viscosity of the blends.

Thermal Properties of PLAC/TPU Blends. Figure 6 shows the DSC thermograms of PLA and the PLAC/TPU blends obtained by increasing the temperature from 0 to 250 ℃ at 10 ℃/min. The melting temperature (T_m) of PLA is approximately 169.68 ℃. In addition, the T_m value of PLAC/TPU is 164-165 ℃. The glass transition temperature (T_g) of PLA is approximately 60.65 ℃. Similar shapes of the T_g curves are reported in the literature.[41-43] Note that the T_g values of the PLAC0.5/TPU and PLAC3/TPU blends are 56.83 and 49.83 ℃, respectively. The decrease in T_g indicates that cardanol effectively improves the compatibility of the PLAC/TPU blends. Similarly, cardanol significantly increases the number of imperfect crystals in PLA.[44] This behavior may be associated with the fact that the cardanol grafted onto PLA disturbs the crystallization of PLA and weakens the interaction of PLA macromolecules owing to the increase in the chain distance. Therefore, the polymer chains interspersed between PLA and TPU reduce the interfacial tension and improve the interfacial adhesion and compatibility of the blends.[31,45]

Mechanical Properties of PLAC/TPU Blends. Figure 7(a) presents images of the FDM-printed dumbbell-shaped specimens of PLA and the PLAC/TPU blends. Warpage, dis-
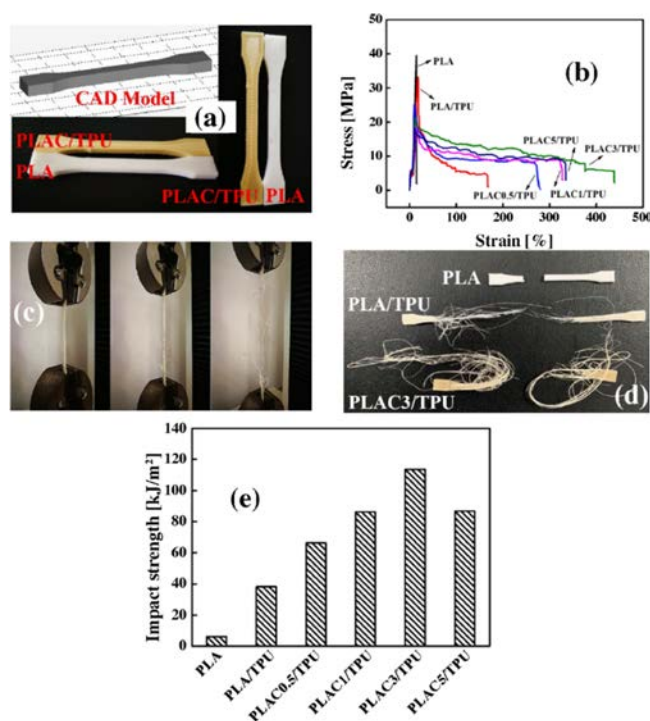
Figure 7. (a) Images of FDM-printed dumbbell-shaped specimens; (b) stress–strain curves of various specimens; (c) deformation sequence of 3D-printed PLAC3/TPU blend after loading; (d) 3D-printed PLA, PLA/TPU, and PLAC/TPU specimens after breaking; (e) impact strength of different blends.

clear yielding characteristics upon stretching (Figure 7(c)). After yielding occurs, the strain increases, whereas the stress is approximately constant. Neck formation for different materials are shown in Figure 7(d). PLA shows the commonly observed brittle behavior of elongation at break, while PLAC/TPU exhibits excellent flexibility through significant yield and neck formation before the fracture occurs, and this is supported by the stress-strain curve shown in Figure 7(b) and the deformation sequence shown in Figure 7(c). This indicates a transition from the brittle behavior of PLA to the ductile behavior of PLAC/TPU. Notably, the elongation at break increases with the cardanol concentration. PLAC3/TPU has a relatively high elongation at break of 439.33% (28 and 1.6 times higher than those of the PLA and PLA/TPU blends, respectively), and its tensile strength is 21.4 MPa. In addition, the impact strength of the blends increases with the cardanol concentration (Figure 7(e)). PLAC3/TPU shows the maximum impact strength, which confirms that cardanol is an excellent agent for toughening PLA/TPU through radical-induced grafting although PLAC5/TPU has the highest MFI (Figure 5(b)). This feature can improve the miscibility and entanglement of the TPU macromolecules in the PLA matrix. The optimum blend is identified as PLAC3/TPU. For a better comparison of the samples, we summarize our results in Table 3.

Conclusions

Cardanol was successfully grafted onto PLA molecule chains under initiation by DCP, and the grafting ratio increased with the cardanol concentration. As the cardanol concentration increased, the T_g and T_m values of the PLAC/TPU blends decreased, and the cold-crystallization peak (T_{cc}) disappeared, indicating good compatibility between PLA and TPU after cardanol grating. In addition, the MFI and tensile strength of the PLAC/TPU blends decreased, whereas the elongation at break and impact strength increased. These behaviors indicated that the cardanol grafting on PLA effectively improved the comprehensive properties of PLAC/TPU. The elongation at break of the 3D-printed specimens of the PLAC/TPU blends was 28 and 1.6 times higher than that of PLA and the PLA/TPU blends,

tortion, and delamination are not observed in any specimen, which shows the good printability of the PLAC/TPU-based filaments. However, the surface quality of the PLA specimen is better than that of the PLAC/TPU blend specimens because the viscosity of polymer filaments strongly affects the dimensional accuracy of the FDM parts. When the viscosity is low, the height and shape of extruded material paths cannot be precisely controlled.[38] Figure 7(b) shows the typical stress–strain curves of PLA and the PLAC/TPU blends. The behavior of PLA and the PLAC/TPU blends changes from stiff to elastic, and the curves are characterized by a yield point of tensile stress and strain. PLA has rigid and brittle characteristics. It instantly shows an evident yield point followed by failure under tensile load. The tensile strength is 39.49 MPa, and the elongation at break is approximately 14.7%. However, the PLAC/TPU blends exhibit

Table 3. Summarize Mechancial Properties of Specimens

Properties	PLA	PLA/TPU	PLAC0.5/TPU	PLAC1/TPU	PLAC3/TPU	PLAC5/TPU
Tensile strength (MPa)	39.49 ± 0.995	32.48 ± 1.95	26.08 ± 1.52	21.23 ± 2.41	21.40 ± 0.995	18.75 ± 1.49
Elongation at break (%)	14.70 ± 1.95	159.13 ± 8.24	255.33 ± 25.95	308.99 ± 9.14	439.33 ± 55.35	305.33 ± 14.37
Impact strength (kJ/m²)	6.144 ± 1.81	38.21 ± 8.83	66.25 ± 9.18	86.20 ± 7.04	113.58 ± 13.24	86.67 ± 7.08

respectively. However, the low surface roughness of the printed parts limits their applicability. Base on the literature, the reactive compatibilizers used for the compatibilization of PLA and TPU are mainly isocyanates and acrylates derivatives. The toxicity of these compatibilizers destroy the biocompatibility of the blends. However, cardanol is an eco-friendly and renewable resource for biocompatibility.[46] The presence of bi-functional and reactive groups in the cardanol structure renders it suitable for introduction into PLA/TPU blends as a reactive compatibilizer. However, the low surface roughness of the printed parts needs to be improved using a post-polishing process if the customized 3D printing design requires good surface quality. Furthermore, different grades of PLA, TPU, or other types of eco-friendly compatibilizers would help achieve superior surface qualities without any extra post processing, and this will be addressed in future studies.

Conflict of Interest: The authors declare that there is no conflict of interest.

References

1. Lopes, L.; Silva, A.; Carneiro, O. Multi-material 3D printing: The Relevance of Materials Affinity on the Boundary Interface Performance. *Addit. Manuf.* 2018, 23, 45-52.

2. Brenken, B.; Barocio, E.; Favaloro, A.; Kunc, V.; Pipes, R. B. Fused Filament Fabrication of Fiber-reinforced Polymers: A Review. *Addit. Manuf.* 2018, 21, 1-16.

3. Han, P.; Tofangchi, A.; Deshpande, A.; Zhang, S; Hsu, K. An Approach to Improve Interface Healing in FFF-3D Printed Ultem 1010 Using Laser Pre-deposition Heating. *Procedia. Manuf.* 2019, 34, 672-677.

4. Tümer, E. H.; Erbil, H. Y. Extrusion-based 3d Printing Applications of Pla Composites: A Review. *Coatings* 2021, 11, 390.

5. Siegkas, P. Dimensional Considerations on the Mechanical Properties of 3D Printed Polymer Parts. *Polym. Test.* 2020, 90, 106656.

6. Parandoush, P., Lin, D. A Review on Additive Manufacturing of Polymer-fiber Composites. *Compos. Struct.* 2017, 182, 36-53.

7. Zhao, F.; Huang, H. X.; Zhang, S. D. Largely Toughening Biodegradable Poly(lactic acid)/thermoplastic Polyurethane Blends by Adding MDI. *J. Appl. Polym. Sci.* 2015, 132.

8. Hashima, K.; Nishitsuji, S.; Inoue, T. Structure-properties of Super-tough PLA Alloy with Excellent Heat Resistance. *Polymer* 2010, 51, 3934-3939.

9. Sivalingam, G., Vijayalakshmi, S.; Madras, G. Enzymatic and Thermal Degradation of Poly(ε-caprolactone), Poly(D,L-lactide), and Their Blends. *Ind. Eng. Chem. Res*. 2004, 43, 7702-7709.

10. Li, K.; Peng, J.; Turng, L. S.; Huang, H. X. Dynamic Rheological Behavior and Morphology of Polylactide/poly(butylenes adipate-co-terephthalate) Blends with Various Composition Ratios. *Adv. Polym. Technol.* 2011, 30, 150-157.

11. Al-Itry, R.; Lamnawar, K.; Maazouz; A. Rheological, Morphological, and Interfacial Properties of Compatibilized PLA/PBAT Blends. *Rheol. Acta* 2014, 53, 501-517.

12. Liu, H.; Chen, F.; Liu, B.; Estep, G.; Zhang, J. Super Toughened Poly(lactic acid) Ternary Blends by Simultaneous Dynamic Vulcanization and Interfacial Compatibilization. *Macromolecules* 2010, 43, 6058-6066.

13. Liu, H.; Song, W.; Chen, F.; Guo, L.; Zhang, J. Interaction of Microstructure and Interfacial Adhesion on Impact Performance of Polylactide (PLA) Ternary Blends. *Macromolecules*. 2011, 44, 1513-1522.

14. Wu, N.; Zhang, H; Fu, G. Super-tough Poly(lactide) Thermoplastic Vulcanizates Based on Modified Natural Rubber. *ACS Sustain. Chem. Eng.* 2016, 5, 78-84.

15. Stokes, K.; McVenes, R.; Anderson, J. M. Polyurethane Elastomer Biostability. *J. Biomater. Appl.* 1995, 9, 321-354.

16. Li, Y.; Shimizu, H. Toughening of Polylactide by Melt Blending with a Biodegradable Poly(ether) Urethane Elastomer. *Macromol. Biosci.* 2007, 7, 921-928.

17. Dogan, S. K.; Reyes, E. A.; Rastogi, S.; Ozkoc, G. Reactive Compatibilization of PLA/TPU Blends with a Diisocyanate. *J. Appl. Polym. Sci*. 2014, 131, 40251.

18. Samantarai, S.; Nag, A.; Singh, N.; Dash, D.; Basak, A.; Nando, G. B.; Das, N. C. Cardanol Functionalized Carboxylated Acrylonitrile Butadiene Rubber for Better Processability, Technical Properties and Biocompatibility. *J. Polym. Environ.* 2019, 27, 1878-1896.

19. Chen, Q.; Xue, H.; Lin, J. Preparation of Polypropylene-graft-cardanol by Reactive Extrusion and Its Composite Material with Bamboo Powder. *J. Appl. Polym Sci*. 2010, 115, 1160-1167.

20. Wang, P.; Liu, J.; Chi, C.; Zhang, Y.; Chen, D.; Chen, Q. Solvent-free Synthesis, Plasticization and Compatibilization of Cardanol Grafted Onto Liquid Isoprene Rubber. *Compos. Sci. Technol.* 2021, 215, 109027.

21. Rigoussen, A.; Verge, P.; Raquez, J. M.; Habibi, Y.; Dubois, P. In-depth Investigation on the Effect and Role of Cardanol in the Compatibilization of PLA/ABS Immiscible Blends by Reactive Extrusion. *Eur. Polym. J.* 2017, 93, 272-283.

22. Tang, H.; Zhou, L.; Bian, X.; Wang, T.; Feng, L; Zhang, B.; Liu, Y.; Chen, X. Highly Toughened Poly(lactic acid) Blends Plasticized by Cardanol in Presence of Dicumyl Peroxide. *Mater. Lett.* 2022, 313, 131777.

23. Huang, Y.; Zhang, C.; Pan, Y.; Wang, W.; Jiang, L.; Dan, Y. Study on the Effect of Dicumyl Peroxide on Structure and Properties of Poly(lactic acid)/natural Rubber Blend. *J. Polym. Environ.* 2013,

21, 375-387.

24. Vikram, T.; Nando, G. Synthesis and Characterization of Cardanol-grafted Natural Rubber—The Solution Technique. *J. Appl. Polym. Sci*. **2007**, 105, 1280-1288.

25. Mohapatra, S.; Nando, G. B. Chemical Modification of Natural Rubber in the Latex Stage by Grafting Cardanol, a Waste from the Cashew Industry and a Renewable Resource. *Ind. Eng. Chem. Res*. **2013**, 52, 5951-5957.

26. Li, L.; Li, B. Rheology, Morphology and Mechanical Property Relationship of Non-halogen Flame Retarded Glass Fibre Reinforced Polyamide 66. *Polym. Polym. Compos*. **2011**, 19, 603-610.

27. Zadhoush, A.; Reyhani, R.; Naeimirad, M. Evaluation of Surface Modification Impact on PP/MWCNT Nanocomposites by Rheological and Mechanical Characterization, Assisted with Morphological Image Processing. *Polym. Compos*. **2019**, 40, E501-E510.

28. Baimark, Y.; Kittipoom, S. Influence of Chain-extension Reaction on Stereocomplexation, Mechanical Properties and Heat Resistance of Compressed Stereocomplex-polylactide Bioplastic Films. *Polymers* **2018**, 10, 1218.

29. Wei, L.; McDonald, A. G.; Stark, N. M. Grafting of Bacterial Polyhydroxybutyrate (PHB) Onto Cellulose *via* in situ Reactive Extrusion with Dicumyl Peroxide. *Biomacromolecules* **2015**, 16, 1040-1049.

30. Liu, J.; Jiang, H.; Chen, L. Grafting of Glycidyl Methacrylate Onto Poly(lactide) and Properties of PLA/starch Blends Compatibilized by the Grafted Copolymer. *J. Polym. Environ*. **2012**, 20, 810-816.

31. Chow, W.; Tham, W.; Seow, P. Effects of Maleated-PLA Compatibilizer on the Properties of Poly(lactic acid)/halloysite Clay Composites. *J. Thermoplast. Compos. Mater*. **2013**, 26, 1349-1363.

32. Greco, A.; Ferrari, F. Thermal Behavior of PLA Plasticized by Commercial and Cardanol-derived Plasticizers and the Effect on the Mechanical Properties. *J. Therm. Anal. Calorim*. **2021**, 146, 131-141.

33. Rytlewski, P.; Żenkiewicz, M.; Malinowski, R. Influence of Dicumyl Peroxide Content on Thermal and Mechanical Properties of Polylactide. *Int. Polym. Process*. **2011**, 26, 580-586.

34. Hu, Y.; Zhu, G.; Zhang, J.; Huang, J.; Yu, X.; Shang, Q.; An, R.; Liu, C.; Hu, L.; Zhou, Y. Rubber Seed Oil-Based UV-Curable Polyurethane Acrylate Resins for Digital Light Processing (DLP) 3D Printing. *Molecules* **2021**, 26, 5455.

35. Natarajan, M.; Murugavel, S. Synthesis, Spectral and Thermal Degradation Kinetics of Novolac Resins Derived from Cardanol. *High Perform. Polym*. **2013**, 25, 685-696.

36. Chieng, B. W.; Azowa, I. N.; Yunus, W. M. Z. W.; Hussein, M. Z. Effects of Graphene Nanopletelets on Poly(lactic acid)/poly (ethylene glycol) Polymer Nanocomposites. *Adv. Mat. Res*. **2014**, 1024, 136-139.

37. Mele, G; Bloise, E.; Cosentino, F.; Lomonaco, D.; Avelino, F.; Marcianò, T.; Massaro, C.; Mazzetto, S. E.; Tammaro, L.; Scalone, A. G. Influence of Cardanol Oil on the Properties of Poly(lactic acid) Films Produced by Melt Extrusion. *ACS Omega* **2019**, 4, 718-726.

38. Gao, X.; Zhang, D.; Qi, S.; Wen, X.; Su, Y. Mechanical Properties of 3D Parts Fabricated by Fused Deposition Modeling: Effect of Various Fillers in Polylactide. *J. Appl. Polym Sci*. **2019**, 136, 47824.

39. Turner, B. N.; Gold, S. A. A Review of Melt Extrusion Additive Manufacturing Processes: II. Materials, Dimensional Accuracy, and Surface Roughness. *Rapid Prototyp. J*. **2015**, 21, 250-261.

40. Boger, D. V. Demonstration of Upper and Lower Newtonian Fluid Behaviour in a Pseudoplastic Fluid. *Nature* **1977**, 265, 126-128.

41. Bhandari, S.; Lopez-Anido, R. A.; Gardner, D. J. Enhancing the Interlayer Tensile Strength of 3D Printed Short Carbon Fiber Reinforced PETG and PLA Composites *via* Annealing. *Addit. Manuf*. **2019**, 30, 100922.

42. Chen, J. M.; Tseng, Y, Y.; Lee, D.; Lee, D.; Lin, Y. T.; Lin, S. H.; Lee, T. Y.; Liu, S. J.; Ito H. A Robust Experimental Model to Explore the Three-dimensional Printing of Polylactide Parts: Solution Versus Melt Extrusion. *Appl. Sci*. **2020**, 10, 509.

43. Wang, S.; Xu, Q.; Li, F.; Dai, J.; Jia, H.; Xu, B. Preparation and Properties of Cellulose-based Carbon Microsphere/poly(lactic acid) Composites. *J. Compos. Mater*. **2014**, 48, 1297-1302.

44. Mo, X. Z.; Wei, F. X.; Tan, D. F.; Pang, J. Y.; Lan, C. B. The Compatibilization of PLA-g-TPU Graft Copolymer on Polylactide/ thermoplastic Polyurethane Blends. *J. Polym. Res*. **2020**, 27, 33.

45. Dong, W.; Wang, H.; He, M.; Ren, F.; Wu, T.; Zheng, Q.; Li, Y. Synthesis of Reactive Comb Polymers and Their Applications as a Highly Efficient Compatibilizer in Immiscible Polymer Blends. *Ind. Eng. Chem. Res*. **2015**, 54, 2081-2089.

46. Fontana, A.; Guernelli, S.; Zaccheroni, N.; Zappacosta, R.; Genovese, D.; De Crescentini, L.; Riela, S. Micellization Properties of Cardanol as a Renewable co-surfactant. *Org. Biomol. Chem*. **2015**, 13, 9214-9222.